Rice

RESEARCH Open Access

The Ratio of A_{400}/A_{1800} Mapping Identifies Chromosomal Regions Containing Known Photoprotection Recovery-Related Genes in Rice

Shoumik Saha[1†], Nilanjan Sinha Mahapatra[1†], Kriti Bhattacharya[1], Rimpa Kundu[1], K. Nimitha[1], Shamba Ganguly[1], Sebantee Ganguly[1], Tirthankar Biswas[1], Prabir K Bhattacharyya[1] and Somnath Bhattacharyya[1*]

Abstract

The rice, like other plants, undergoes photoprotection mode by increasing nonphotochemical quenching (NPQ) in high light intensity (> 1200 µmol $m^{-2}s^{-1}$ PPFD), which attenuates photosystem II yield (φPSII) drastically. The plant remains in photoprotection mode even after light intensity becomes not stressful for an extended period. While there are significant differences in the time it takes for photoprotection to recover among different genotypes, its use is limited in plant breeding because measuring the chlorophyll fluorescence parameters in progressive actinic light after dark adaptation takes more than forty-five minutes per genotype. The study finds that instantly measured A_{400}/A_{1800} ratio by five minutes in flag leaves of 25 diverse genotypes strongly associated with the $\varphi PSII_{400}$ differences between theoretical and actual, qPd_{400} and NPQ_{400} with R^2 values 0.74, 0.65 and 0.60, respectively. In two consecutive years, GWAS of A_{400}/A_{1800} ratio identified the regions with genes reported earlier for plant photoprotection recovery. Additionally, QTL analysis in a RIL population also identified the regions carrying known genes related to photoprotection. Thus, the A_{400}/A_{1800} ratio can quickly phenotype many plants for easier introgression of the traits in popular cultivars. The identified genotypes, genes, and QTLs can be used to improve yield potential and allele mining.

Keywords Rice, Chlorophyll-fluorescence, Fluctuating light, Photoprotection, Photosynthesis

†Shoumik Saha and Nilanjan Sinha Mahapatra contributed equally to this work.

*Correspondence:
Somnath Bhattacharyya
somnathbhat@yahoo.com
[1]Crop Research Unit, Genetics and Plant Breeding, Bidhan Chandra Krishi Viswavidyalaya, Mohanpur 741252, India

Introduction

Rice is a primary source of carbohydrates with low fat, essential amino acids, vitamins, and minerals. It accounts for 20% of the global calorie consumption and 35–60% of calorie intake in Asia (Abdullah et al. 2006). For the food security of this ever-increasing global population with limited agricultural land and multiple environmental stresses, there is an urgent need for a quantum yield jump in rice production and productivity. Over the past half-century, the potential yield of rice has been primarily increased through improvements in the harvest index, stress tolerance and enhanced responses to additional nitrogen fertilizers (Long et al. 2006). However, the harvest index has a theoretical maximum limited by the source and sink relationship (Smith et al. 2018). Recent research indicates that a balance between the source and sink factors is crucial for plant growth (Jonik et al. 2012; Rossi et al. 2015). To overcome the yield barrier in rice production, the key components are strengthening 'source production' and 'sink utilisation' (Sonnewald and Fernie 2018). In this context, the role of photosynthesis in improving yield potential is gaining renewed importance (Foyer et al. 2017). Despite a weak correlation between photosynthesis and yield in optimal conditions, enhancing photosynthetic efficiency in various abiotic stress situations can directly improve yield (Fischer and Edmeades 2010; Reynolds et al. 2009; Ambavaram et al. 2014; Kromdijk et al. 2016; Muhammad et al. 2021; Makino 2021; Amin et al. 2022).

Photosynthesis is a light-dependent process where light energy is captured and converted to chemical energy. This process converts around 5–30% of the absorbed light energy into chemical energy. However, rapidly changing light conditions caused by cloudy weather, seasonal variation, geographic location, mutual shading of leaves, and the angle of the sun throughout the day can reduce photosynthetic efficiency and carbon gain. This can result in field crops losing up to 20% of their potential yield (Kromdijk et al. 2016). To optimise photosynthesis, plants have evolved a plethora of adaptive, photo acclamatory and photoprotective mechanisms to deal with such dynamic field conditions as fluctuating light intensity ranges 400 μmol m^{-2} s^{-1} to 1800 μmol m^{-2} s^{-1} (Ganguly et al. 2020). In field conditions when plants receive higher light intensities, to protect themselves from photodamage and photoinhibition, it dissipates the excess light energy absorbed by light-harvesting complexes (LHC) as heat from photosystem II (PS II) and trimeric LHC II subunit by a mechanism known as non-photochemical quenching (NPQ) (Ruban 2016; Muller et al. 2001). However, this process is slower to recover than it is to activate; as a result, the PSII antennae recover from the quenched to the unquenched state at a slower pace, leading to a temporary suppression of the photosynthetic quantum yield of CO2 fixation upon transitioning from high to low light intensity. Simulation models have estimated losses of CO2 fixation ranging between 7.5% and 30% for crop canopies over a diurnal course (Kromdijk et al. 2016). To combat this, researchers have suggested plants with a quicker recovery rate from NPQ to improve crop photosynthetic efficiency and increase yields (Kromdijk et al. 2016; De Souza et al. 2022).

Based on relaxation kinetics in darkness following a period of illumination, NPQ is divided into several components (qE, qZ, qI, qT, qH, qM) (Bassi et al., 2021; Kromdijk et al. 2016; Giovagnetti et al., 2015; Matuszyńska et al. 2016; Ruban 2016; Tietz et al. 2017). Among these six components, qE is the strongest, quickest and most effective component in terms of rapid formation in high light (0.5–2 min) and rapidly reversible in low light (Kromdijk et al. 2016; Bassi et al., 2021). qZ component takes 10–15 min for relaxation and is linked to the kinetics of the zeaxanthin pool (Giovagnetti et al., 2015; Matuszyńska et al. 2016). Another component of NPQ that results from photo-inhibitory damage to PSII reaction centres is qI (Takahashi et al., 2011). It takes longer (more than hours) for recovery through an as-yet unidentified mechanism (Takahashi et al., 2011). The primary function of the fourth component, qT, is balancing light absorption between the two photosystems in conditions of low light (Rochaix et al., 2007). qH is a sustained Chl fluorescence quenching component, i.e., it relaxes very slowly (decay time > 30 min) independent from PSII RC damage and qM is a decline in Chl fluorescence yield (decay time~20–30 min), which arises from the light-induced chloroplasts photo relocation within the cell (Bassi et al., 2021).

NPQ is a quantitative trait controlled by many genes and QTLs like *OsPsbS1* (Os01g0869800), *OsPsbS2* (Os04g0690800), *OsVDE* (Os04g0379700), *OsZEP* (Os04g0448900), *OsPGR5* (Os08g0566600), *OsPGRL1A* (Os08g0526300), *OsPGRL1B* (Os03g0857400), *OsLUT1A* (Os10g0546600), *OsLUT1B* (Os02g0817900), *OsLUT1C* (Os02g0173100), *OsLUT2* (Os01g0581300), *HQE1* (high qE 1, for high energy-dependent quenching 1) and *HQE2* (Kasajima et al. 2011; Wang et al. 2017). Among those, *PsbS1* is a major gene with *VDE* and *ZEP*, which control NPQ variation through the Xanthophyll Cycle (Kromdijk et al. 2016; Fu et al. 2021; Moya Clark 2023).

Chlorophyll fluorescence measurement is the most popular technique for getting information about PSII activity to understand photosynthetic mechanisms in different biotic and abiotic stresses and plants' response to environmental changes. Though from chlorophyll fluorescence, a large number of parameters like non-photochemical quenching (NPQ), the maximum quantum efficiency of photosystem II (Fv/Fm), the quantum yield of PSII (ΦPSII), photoinhibition measurement as

a decline in the quantum coefficient of photochemical quenching (qP) in the dark, measured immediately after illumination (qPd). For all these measurements, a basic requirement is a dark adaptation of the leaf for a minimum of 25–30 min, which can also vary according to the plant species (Murchie et al., 2013). In field conditions, adopting leaves in the dark for a period of 25–30 min and then measuring data in replications for many samples is time-consuming and laborious. Thus, screening a large, segregating population to select the desired line is almost impossible. As a result, despite the good association between yield and the quick photoprotection recovery ability, its use in yield, biomass enhancement and allele mining is not so useful. Thus, an alternate, easy-to-use methodology is needed to improve the rice plant's source strength. In this study, instantly measuring A_{400} and A_{1800} ratios showed a good correlation with several quick photoprotection recovery traits, and mapping by GWAS and QTL analysis identified the chromosomal regions which carry previously reported genes for the photoprotection in plants.

Materials and Methods

Growing Plants and Measuring Biomass and Yield

A panel of 96 diverse rice genotypes/accessions comprising landraces, aus, aromatic, and released cultivars were used along with 130 RILs from a cross between Swarnaprabha (SP) and IR64 (Supplementary Tables 2 and Supplementary Table 5). The naturally diverse population and subpopulation were considered to ensure that the association between SNP-based allelic diversity and the A400/A1800 ratio is true. However, a RIL population developed from two parents with contrasting A400/A1800 ratios was used to identify the QTLs controlling the ratio. The purpose is to confirm that the loci identified in association analysis from the natural population are similar also in RILs. As the RIL population was chosen after the selfing of nine generations, there was sufficient scope for recombination between all loci that the two parents differed. Thus, even after nine generations of recombination, the chances of false discovery are negligible if the trait (here A400/A1800) links with the polymorphic SNPs. Most of the photosynthetic metrics between the two parents differ significantly other than a few, which are taken at 1800 μmol $m^{-2}s^{-1}$ PPFD.

The experiment was conducted at the University Instructional Farm (22.97°N and 88.43°E), situated in the New Gangetic alluvial zone of Nadia District, West Bengal, India. Twenty-five diverse genotypes were initially grown in an earthen pot with a 28 cm diameter and 10 lt capacity in RBD with three replications. The diverse set of 96 genotypes and RIL population were planted in three rows of 10 m long with 20×15 cm spacing in randomized block design in wet seasons 2018, 2019 and 2023, respectively. The RIL population was developed by the single seed descent method from the F2 population of SP X IR64 and advanced to F7 before phenotyping and genotyping. Recommended doses of NPK that is @100:60:40 kg/ha were used, and 25 days seedlings were transplanted. Ten randomly selected plants from three rows of each line of the RIL population of each replication were used for biomass and yield estimation. After harvesting, threshing and oven drying at 32℃ (to moisture content 14%) per plant grain yield was recorded as g/plant. The plant samples without panicles (straw part) were oven-dried at 70℃ and weighed, then summed up with grain yield and recorded as total biomass g/plant. An average of 10 plants were considered as a single replication.

Gas Exchange and Chlorophyll Fluorescent Measurement

Photosynthetic parameters and chlorophyll fluorescence measurements were done simultaneously/together by using the LiCor portable gas exchange system (LI-6800, Li-Cor, Lincoln, NE, USA) with chlorophyll fluorescent measuring attachment. 8–10 days old flag leaves were considered for photosynthetic parameters and chlorophyll fluorescence measurements. The widest part of the flag leaves was considered for recording observations. Data were taken between 9.00 and 13.00 h when external light intensity varied between 1000 and 1300 μmol $m^{-2}s^{-1}$ PPFD. LI-6800 cuvette allows air temperature of 28℃, CO_2 concentration of 400 ppm, and relative humidity of 65%. In the pot experiment, three flag leaves of each plant were taken for observation recording in each replication. Plants were dark-adopted for 30 min in a dark chamber. Then dark adopted leaves were placed inside the LI-6800 cuvette without giving any actinic light (AL), and a measuring light (MB) was applied to measure minimum fluorescence (Fo), then a saturating flash of light also called saturating pulse (SP) was applied to measure maximum fluorescence at dark (Fm), and the difference between them (Fm – Fo) gives variable fluorescence (Fv) as well as Fv/Fm confer maximum quantum efficiency of photosystem II. After dark adopted measurements, the actinic light illumination procedure was chosen as follows: a leaf was illuminated with 11 phases of progressively increasing and decreasing light intensities of 200, 400, 600, 1000, 1500, 1800, 1500, 1000, 600, 400, 200 μmol $m^{-2}s^{-1}$ for 5 min (interval time) for each PPFD. This light exposure is more natural for the plant than abrupt exposure to a single light intensity, especially at nearly saturating levels. The measurements for NPQ, PSII yield and qPd have been performed in the dark for 3 s after switching the actinic light at the end of each illumination phase using 2–3 consecutive saturated pulses. Each pulse was followed by a ~ 7-second period of far red light illumination in the dark (Ruban and Murchie 2012).

The programmed illumination procedure was: (SP)–(AL on)–(5 min)–(SP)–(AL off/FR on)–(10 s)–(SP)–(5 s)–(AL on/FR off)–repeat, where AL, SP and FR represent actinic light, saturating pulse and far red light respectively All these operations were programmed before placing the leaves inside the cuvette in automatic LI-6800. Except qPd all the photosynthetic parameters and chlorophyll fluorescence measurements were retrieved from the machine. qPd is a measure of photoinhibition. qPd value 1 denotes the absence of photoinhibition, and qPd values < 1 imply the presence of photoinhibition, indicating divergence of theoretical and actual yield of PSII. qPd is calculated according to the following equation (Ruban and Murchie 2012)

$$\mathrm{qPd} = \frac{\mathrm{Fm'} - \mathrm{Fo'act.}}{\mathrm{Fm'} - \mathrm{Fo'cal.}} \quad (1)$$

For calculating Fo'calc. we have used the formula given by Oxborough and Baker (1997).

Fo' calc.

$$= \frac{1}{\left(\frac{1}{\mathrm{F0}} - \frac{1}{\mathrm{Fm}} + \frac{1}{\mathrm{Fm'}}\right)} \quad (2)$$

A_{1800} was measured in the flag leaves of field-grown plants with actinic light illumination of 1800 µmol $m^{-2}s^{-1}$ for 3 min, followed by low light illumination of 400 µmol $m^{-2}s^{-1}$ for 2 min. The mean of five plants was considered for one replication. The ratio was calculated simply by dividing A_{400}/A_{1800}.

Genome Wide Association Analysis

7 K SNP chip was utilised to genotype the 96 diverse genotypes and 130 RILs (Thomson et al., 2017, Morales et al., 2020). For GWAS, out of 7098 SNPs, SNPs with minor allele frequency (MAF) of less than 10% and more than 10% missing data were removed. Finally, 1840 SNPs were imputed using the LD-kNNi method (Money et al. 2015) in Tassel 5 using 30 nearest neighbors (Supplementary Table 6). All 1840 SNPs were used to build up a phylogenetic tree using UPGMA (Unweighted Pair Group Method with Arithmetic Mean). PCA analysis was done using R software (version 4.2.0) and the GAPIT (Genomic Association and Prediction Integrated Tool) package. All 1840 SNPs were used for estimation of population structure with STRUCTURE software (Pritchard et al. 2000), which use a Bayesian clustering method. A structure harvester was used to determine the optimum value of K, which calculates the Evanno delta K value by plotting the LnP(D) value vs. K (Earl & vonHoldt 2012). Linkage disequilibrium (LD) among the genome-wide polymorphic markers was created with a sliding window size of 50 markers. The obtained r^2 values were graphed against physical distances, and a LOESS curve was applied to visualize the decay of linkage disequilibrium (LD). The LD decay distance was estimated using the approach developed by Hill and Weir (1988) and evaluated at the commonly accepted r^2 threshold of 0.2 (Vos et al., 2017). Further, GWAS (Genome Wide Association Studies) was performed using 'FarmCPU' (Fixed and random model Circulating Probability Unification, Liu et al. 2016) and 'BLINK' (Bayesian information and Linkage-disequilibrium Iteratively Nested Keyway, Huang et al. 2019) methods. The SNP-trait associations were considered significant when P-value < 0.001 and PVE was calculated only for the loci with significant p-value less than 10^{-5}.

QTL Analysis

Out of the total 7098 SNPs, 2268 SNPs exhibited good genotyping data for RILs. Among these, 927 unbiased polymorphic SNPs were considered for mapping purposes. The QTL IciMapping software (Meng et al. 2015) was employed to construct a linkage map using polymorphic 927 SNPs (Supplementary Table 7). This linkage map was then aligned with the physical map and nucleotide positions in the rice genome database, allowing for precise identification of SNP locations regarding nucleotide numbers. To map the traits and derived traits in the mapping population, composite interval mapping (CIM) was utilised, using the mean values of each trait. A LOD (logarithm of odds) score value of 3.0 was considered significant for QTL detection, and QTLs with >10% PVE were classified as major QTLs.

Results

For 25 genotypes, the nonphotochemical quenching (NPQ), the theoretical and actual quantum yield of PSII (ϕPSII), and photoinhibition (qPd) were measured in 1800, 1500, 1000, 600, 400, 200 µmol m^{-2} s^{-1} photoactive radiation (PAR) in five minutes after dark adaptation (Fig. 1).

The NPQ and other parameters differ significantly among the twenty-five genotypes in 1800 or 400 PAR (Supplementary Table 1). The theoretical quantum yield of PSII was simulated for each of the six points. Thus, the difference between theoretical and actual ϕPSII400 indicates the photoprotection recovery ability of the genotypes after twenty minutes. The minimum difference (0.02) between the theoretical and actual quantum yield of PSII, ϕPSII400 (T-A), after twenty minutes, is recorded for genotypes such as Gopalbhog, Shatabdi, and Swarnaprabha, and the maximum difference (0.10–0.12) is observed for Neeroja, Humbla, and Sashi (Fig. 2).

In the steady state, comparing A100-A400 in twenty-five genotypes confirmed the no variation in A100 and a small variation in A200-A300, where the maximum

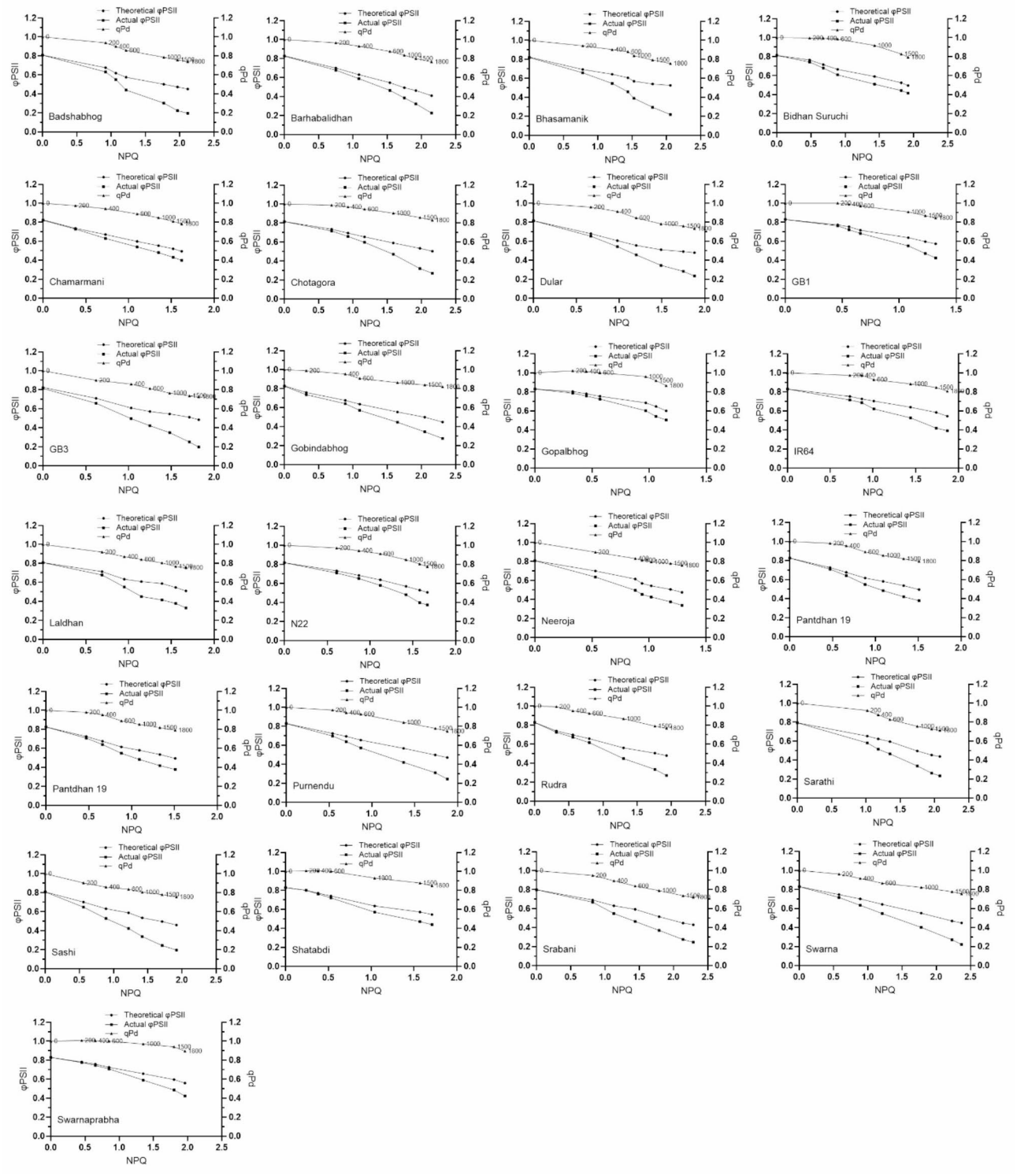

Fig. 1 Graph representing the genotypic specific mean theoretical and actual photosystem II quantum yield/efficiency, φPSII; the nonphotochemical quenching, NPQ; and photoinhibition, qPd; for twenty-five rice genotypes, both in ascending and descending 200, 400, 600, 1000, 1500, and 1800 µmol m^{-2} s^{-1} PPFD, as indicated by six points in each genotype

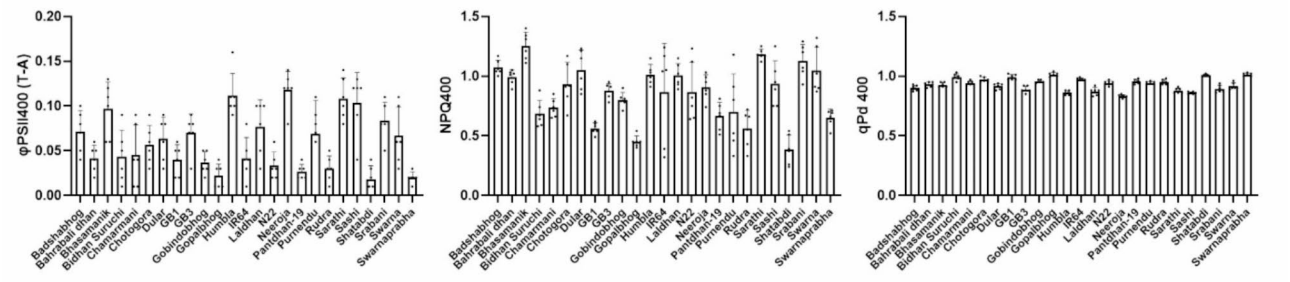

Fig. 2 Bar diagram showing the difference between theoretical and actual PSII yield at 400 µmol $m^{-2}s^{-1}$ PAR [φPSII 400 (T-A)], NPQ400 and qPd400 of 25 genotypes

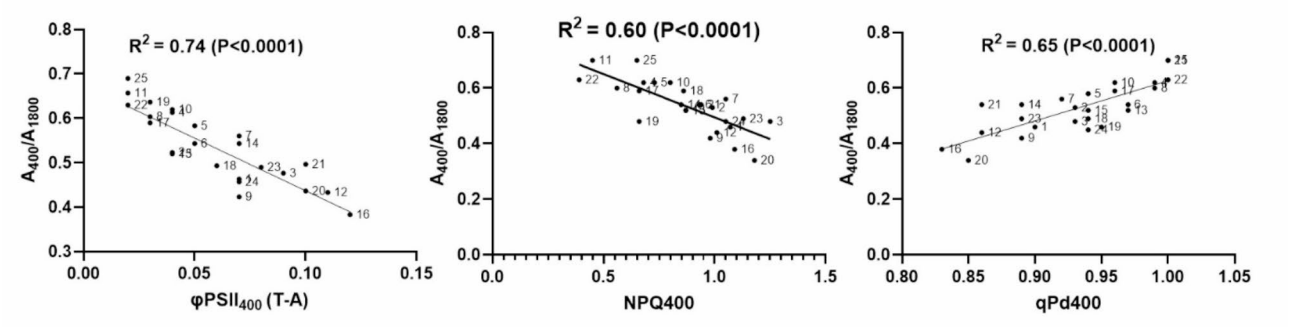

Fig. 3 Simple linear regression curve with equation and R^2 value between A_{400}/A_{1800} with φPSII400 (T-A), NPQ400 and qPd400. The number surrounding the regression line represents the genotype number

variation was at A400 (Supplementary Fig. 1). It was already shown that at A200, there was no gap between theoretical and actual φPSII400 in most genotypes (Fig. 1). As most of the genotypes exceed the light saturation point at 1800 PPFD (Supplementary Fig. 2), the ratios of A1800 and A400 were estimated in the twenty-five genotypes in 5-minute intervals. The ratio differs significantly among the genotypes. A strong association was observed between φPSII400 (T-A) and qPd400, as well as between NPQ400, with R^2 values of 0.74, 0.60, and 0.65, respectively (Fig. 3).

As the earlier result with twenty-five genotypes indicated a good association between the instantly measured A_{400}/A_{1800} ratio and φPSII400 (T-A) and NPQ400, ΦPSII400, and qPd400, a panel of ninety-six genotypes was considered for the association analysis. 7k SNP-based genotypic data confirmed two substructures within the ninety-six genotypes considered in this analysis (Supplementary Fig. 3). Genotypic variations explained almost 68% of total variations. Year-wise variation and interaction are small, 0.1% and 2%, respectively (Supplementary Table 3). In this study, we observed a correlation coefficient (r) between two years, which is 0.87.

Based on the reliability of SNP-based genotyping (7k chip), 1840 SNPs were finally considered for linkage disequilibrium study, and it was sufficiently high to cover the 12 chromosomes. Two years' data and their mean were analysed separately. GWAS identified five genomic locations on four chromosomes, explaining PVE > 5% with a p-value $< 10^{-5}$ in either of the methods (Fig. 4). Among these, two QTNs on chromosome 4 and one on chromosome 9 explained > 10% phenotypic variations (Table 1). In a 100 kb window flanking the locus, four known genes associated with photoprotection were identified when putative genes were searched in RAB-DB. The known genes related to photoprotection recovery, like Lycopene epsilon cyclase (LYCE/LUT2, Os01g0581300), located on chr 01: 22535013.22538645 is very close to the associated SNP, 756842 located on 22601215nt. Similarly, Violaxanthine de-epoxidase (VDE) and Zeaxanthine epoxidase (ZEP) are located on chromosome 4, and Phosphoglycolate phosphatase 2 (PGLP2 (Os09g0261300) is located near the associated marker on chromosome 9 (Supplementary Table 4). The box plot showed the influences of allelic pairs on the traits in all four chromosomal locations (Fig. 5).

QTL Mapping of A400/A1800 Ratio

Two parental differences in photosynthesis and photoprotection-related parameters are given separately (Table 2). However, the A400, A1800, and their A400/A1800 ratio were estimated in five minutes. As described in the methodology section, all other parameters are considered from the data set of 11 phases of progressively increasing and decreasing light intensities at the five-minute interval of each point. Non-significant differences

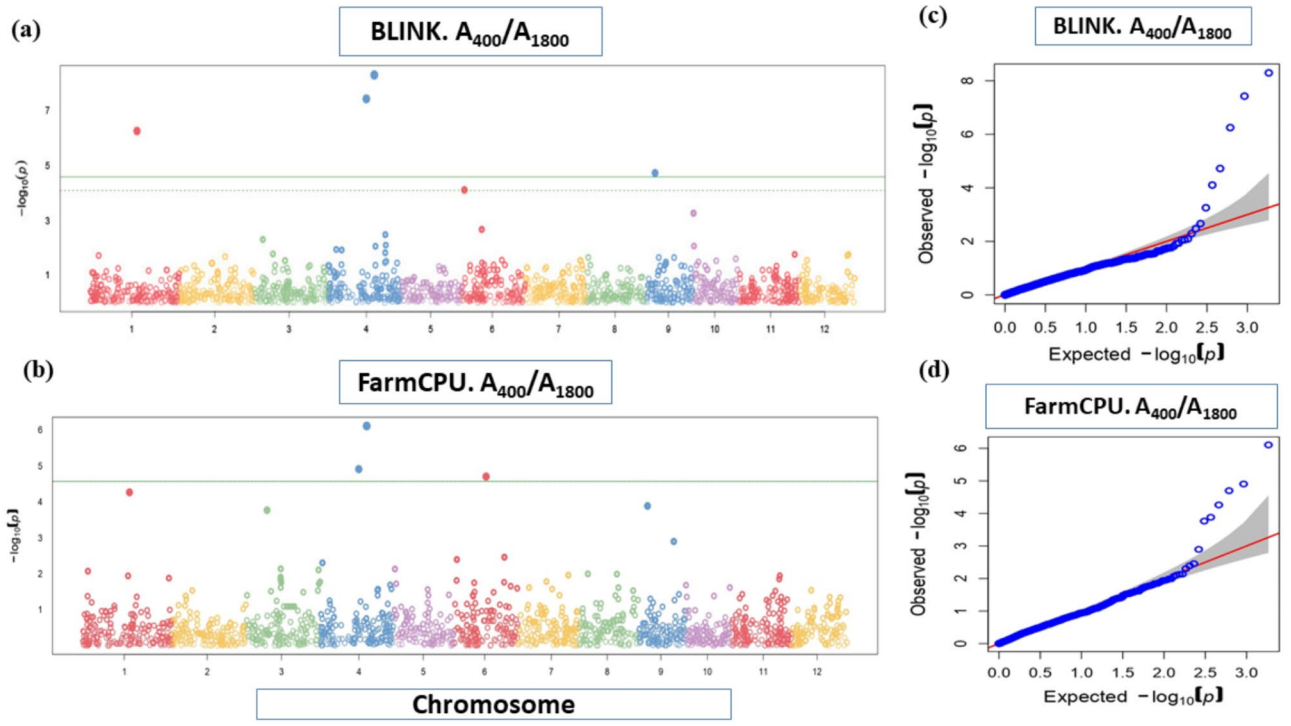

Fig. 4 Using two years of mean data, the Manhattan plots (left) and Q-Q plots (right) for the genome-wide association study of A400/A1800 in the ninety-six panel. For Manhattan plots, -log10 P-values from a genome-wide scan are plotted against the position of the SNPs on each of the 12 chromosomes. For quantile-quantile plots, the horizontal axis shows the -log10-transformed expected P-values, and the vertical axis indicates -log10-transformed observed P-values

between Swarnaprabha and IR 64 were observed for the parameters mostly recorded in saturated light intensity, like A1800, NPQ1800, and theoretical PSII yield at 1800 and 400 PPFD. The wide variation of the A_{400}/A_{1800} ratio was observed among 130 RILs (Supplementary Table 5).

The QTL analysis led to the identification of five QTLs for the A_{400}/A_{1800} ratio. These five QTLs were distributed in four chromosomes, two on chromosome 1 and one each on Chr 4,8,9, contributing to phenotypic variation ranging from 3.86 to 25.28% with LOD values ranging from 3.2 to 16.3 (Supplementary Fig. 4). Three major QTLs explain that more than 10% of PVE are located on chromosomes 1, 4, and 9 (Table 3). A major QTL1.2 between 37.83 Mbp to 38.84 Mbp with LOD 16.32 controlling 25.28% of the phenotypic variation of A_{400}/A_{1800} ratio. One well-known photoprotection-related gene, *PsbS1* (Os01g0869800), is inside the QTL1.2. The QTL on chromosome 4 between 15.94 Mbp to 18.70 Mbp with LOD 8.50 explained 12.56% phenotypic variation and exactly where a previously identified photoprotection recovery gene, Violaxanthine de epoxidase (*VDE*, Os04g0379700) is located. Another two QTLs in chromosomes 8 and 9, explaining 3.9 and 13.95% of the total phenotypic variation and the related known genes, *OsPGRLIA* (Os08g0526300) and *OsbZIP72* (Os09g0456200), are located. Thus, the A_{400}/A_{1800} ratio mapping identified a few QTLs where the known photoprotection recovery genes were reported earlier. Thus, the GWAS and QTL-mapping of the instantly measured A_{400}/A_{1800} ratio in five minutes identified the loci with photoprotection recovery genes, like *OsPsbS1*, *OsVDE*, *OsZEP*, *OsLUT2*, *OsPGRL1A*, *OsbZIP72*. A_{400}/A_{1800} was associated with biomass with an R^2 value of 0.17 (P=<0.0001) in the RIL population (Supplementary Fig. 5). On the other hand, A_{400}/A_{1800} ratio and yield showed a positive association with an R^2 value of 0.11 (P=<0.0001). However, biomass and yield showed a positive association as expected.

Discussion

Once plants enter photoprotection (PP) mode to save the photosystem II-related proteins in high light intensity, they continue for an extended period even though the light intensity is not stressful for photosynthesis. Thus, during fluctuating light environments, until PP recovers, it limits CO_2 assimilation. Plants with quick photoprotection recovery (QPR) ability can improve biomass and yield significantly (Kromdijk et al. 2016; De Souza et al. 2022). The major challenge is PP-phenotyping, which takes almost forty-five minutes and requires complete dark adaptation, making it very difficult for standing crops in the field. However, a new method was proposed without the dark adaptation stage (Tietz et al. 2017),

Table 1 The significant A400/A1800-QTN identified in GWAS in two consecutive years and their mean; a few known genes located near the locations also mentioned

SNP Name	Chromosome and position	Year 1				Year 2				Mean data				Known genes associated with photoprotection
		P- value	PVE (%)	Allele effect	Detected in different methods	*P*- value	PVE (%)	Allele effect	Detected in different methods	*P*- value	PVE (%)	Allele effect	Detected in different methods	
756,842	1.22601215	8.02E-06	5.40	0.02	BLINK	4.53E-05	4.68	0.02	BLINK	5.61E-07	7.63	0.02	BLINK	*LUT2/LYCE*
		1.06E-05	9.26	0.02	F-CPU	0.00072	4.9	0.01	F-CPU	5.49E-05		0.02	F-CPU	(Os01g0581300)
4,333,768	4.18408626	3.00E-06	5.84	-0.02	BLINK	2.98E-07	16.12	-0.03	BLINK	3.75E-08	9.29	-0.03	BLINK	*OsVDE*
		1.36E-07	12.23	-0.03	F-CPU	5.81E-06	18.12	-0.02	F-CPU	1.25E-05	17.83	-0.02	F-CPU	(Os04g0379700)
4,460,072	4.22231867	1.78E-10	7.18	0.03	BLINK	9.26E-06	13.90	0.02	BLINK	5.06E-09	9.07	0.03	BLINK	*OsZEP*
		1.84E-07	9.43	0.02	F-CPU	4.61E-07	8.12	0.02	F-CPU	7.85E-07	10.22	0.02	F-CPU	(Os04g0448900)
id6009055	6.15538142	0.000139	4.93	-0.03	F-CPU	0.000385	3.98	-0.01	BLINK	2.00E-05	5.65	-0.04	F-CPU	*Hsp; H0124E07.4*
						1.14E-06	5.72	-0.03	F-CPU					(Os06g0469800)
c9p4565514	9.4565515	2.51E-05	10.5	-0.04	BLINK	1.76E-06	17.25	-0.05	BLINK	1.89E-05	14.87	-0.04	BLINK	*PGLP2*
		0.00074		-0.03	F-CPU	0.00019	4.81	-0.04	F-CPU	0.000131	9.87	-0.03	F-CPU	(Os09g0261300)

which still involved considerable time and customised equipment.

Preliminarily, twenty-five genotypes were considered to understand the association between photoprotection recovery-related traits (PSII yield, NPQ, qPd) with the instantly measured (5 min) A_{400}/A_{1800} ratio. Rice genotypes were so chosen that aus, aromatic, low-land, high-yielding indica and landraces were present. The study considered all the probable ratios, A200 to A600 by A1800, but the most varied among the 25 genotypes was A_{400}/A_{1800}. The ratio targets measuring the alternate and easier way to estimate any rice genotypes' quick photoprotection recovery ability. The photoprotection ability at 200 or 300 PPFD is negligible, as indicated by almost zero ϕPSII200 (T-A); thus, due to lack of variation, it is not possible for the association analysis considering a more extensive data set. At 1800 µmol $m^{-2}s^{-1}$ PPFD, all genotypes undergo photoprotection almost at the maximum level, as observed from low ϕPSII and qPd with higher NPQ, whereas, at 400 µmol $m^{-2}s^{-1}$, their photoinhibition reaches a minimum but maintained high variations among the genotypes. Contrarily, at 200 and 300 µmol$m^{-2}s^{-1}$, the net photosynthesis rate is almost similar and lacks variations. So, measuring the A_{400}/A_{1800} ratio is justified compared to considering less than 400 PPFD. In tobacco at the steady state, no NPQ differences were observed at below 400PPFD (Kromdijk et al. 2016). They also observed no photoinhibition and a very small amount of photoprotection in plants below 400 PPFD.

In our experiment, it was observed that almost all the 25 genotypes had reached their saturation level at 1500 PPFD, and from 1500 to 1800PPFD, no further significant improvement in the rate of photosynthesis except GB3, N22 and Shatabdi, which showed saturation at 1800 PPFD. Earlier reports also justify our consideration of 1800PPFD as the maximum light intensity (Acevedo-Siaca et al., 2020; et al. 2021). They considered 1700 PPFD to be the maximum highlight intensity of rice. Several genotypes showed a small gap between actual and theoretical PSII yield at 400 µmol$m^{-2}s^{-1}$ PPFD, indicating their quicker photoprotection recovery abilities. Their efficient photoprotection recovery ability was also confirmed by almost qPd-value one at the same point. The multiplicative variable was not considered because the linear relationship between the A400/A1800 ratio and the photosynthesis matrices has a high R^2 value. Also, the data set used in the regression analysis of twenty-five genotypes is not skewed, and to keep the methodology simple, only the ratio was considered, successfully identifying the chromosomal loci with known photoprotection recovery-related genes. Here, the genotypes with quick photoprotection recovery, like, Swarnaprabha, Gopalbhog, Shatabdi, GB1 and Bidhan Suruchi, gave a higher A_{400}/A_{1800} ratio, measured instantly (in 5 min). A_{400}/A_{1800} may

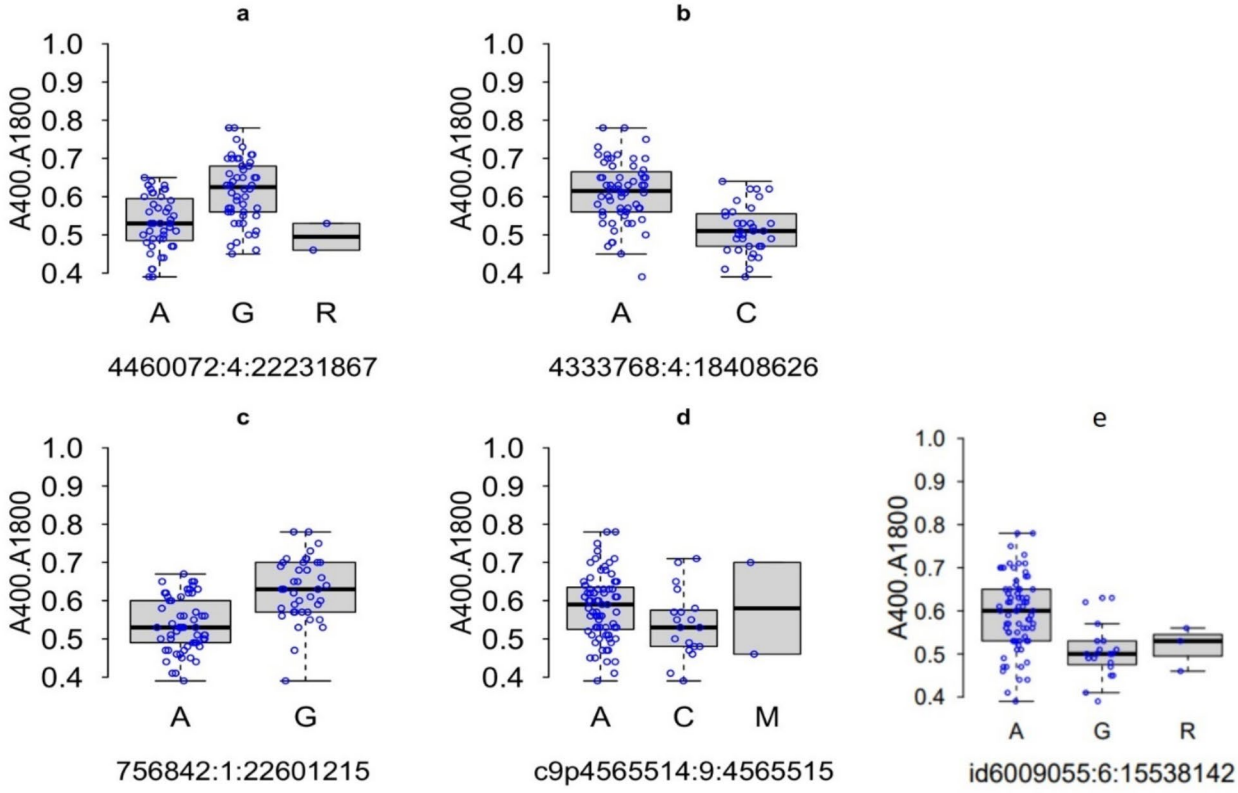

Fig. 5 Box plot showing the allelic effect of the associated SNPs; each line in the box represents mean, R represent heterozygotes (A, G), M represents heterozygote (A, C); the name of the SNPs its chromosomal location and exact nucleotide position are given under each box plot

Table 2 Difference between Swarnaprabha and IR64 in photosynthesis and photoprotection parameters with SD in bracket. Their significance level indicated by *, ** for $p < 0.05$, $p < 0.01$ respectively

Trait	Swarnaprabha	IR64	*P*
A_{400}	14.3 (±0.8)	10.62 (±0.9)	**
A_{1800}	20.35 (±1.6)	20.56 (±2.5)	ns
A_{400}/A_{1800}	0.70 (±0.07)	0.52 (±0.05)	**
NPQ_{400}	0.65 (±0.07)	0.87 (±0.14)	*
NPQ_{1800}	1.96 (±0.19)	1.87 (±0.2)	ns
NPQ_{400}/NPQ_{1800}	0.33 (±0.06)	0.47 (±0.19)	ns
$\Phi PSII_{400\ actual}$	0.75 (±0.02)	0.69 (±0.02)	**
$\Phi PSII_{400\ theoretical}$	0.77 (±0.01)	0.73 (±0.04)	ns
$\Phi PSII_{400\ (theoretical - actual)}$	0.02 (±0.002)	0.05 (±0.02)	*
$\Phi PSII_{1800\ actual}$	0.42 (±0.01)	0.39 (±0.02)	*
$\Phi PSII_{1800\ theoretical}$	0.56 (±0.03)	0.55 (±0.03)	ns
qPd_{400}	1 (±0.01)	0.97 (±0.01)	*
qPd_{1800}	0.90 (±0.02)	0.81 (±0.03)	**

be a good indicator of the PP recovery trait as supported by its positive association with the difference between theoretical and actual $\phi PSII_{400}$, NPQ400, and qPd400. Thus, an instant (5-minute interval) estimated A_{400}/A_{1800} ratio indicates the genotype's quick protection recovery abilities. Here, 8-10-day-old flag leaves were considered for the optimum photosynthesis ability at this stage (Saha et al. 2023). So, before considering the A_{400}/A_{1800} ratio as an indicator of QPR in rice, the ratio was further used for GWAS in a panel of 96 diverse genotypes and QTL analysis using a RIL population developed from a cross between Swarnaprabha and IR64. The A400/A1800 ratio in a flag leaf is highly reproducible if the flag leaf is 5–10 days old, as indicated by year-wise variation, which is small and has a high correlation between the years. It is also worth mentioning that non-significant differences in photosynthetic parameters at saturated light between two parents make their RIL population suitable for mapping their quick photoprotection relaxation abilities.

In addition to the indica landraces and released cultivars, another small subpopulation comprised aus and aromatic genotypes, confirming the accurate genotyping and analysis. GWAS was performed following two models (BLINK, FarmCPU) to reduce false discovery. Only five loci were common between two years of data and their means in both models. Of the four genes near the associated markers, three were related to the Xanthophyll cycle and another critical gene, phosphoglycolate phosphatase (PGLP2), degrades 2-phosphoglycolate (2PG). One 2PG is the final toxic product of RuBP-oxidation, along with one molecule of one 3PGA. Until 2PG degrades, it inhibits photosynthesis by blocking the

Table 3 List of QTLs, left and right markers, their location, LOD score, phenotypic variation (PVE) and additivity for A_{400}/A_{180}

SL. No.	QTLs	Chr	Marker		Position		LOD	PVE (%)	σ^2_A	PP genes present within QTLs
			Left	Right	Left	Right				
1	qA_{400}/A_{1800} 1.1	1	1,163,456	SNP-1.37415410.	35,825,579	37,416,454	5.10	5.32	-0.0296	
2	qA_{400}/A_{1800}1.2	1	SNP-1.37834974.	1,243,398	37,836,018	38,847,770	16.32	25.28	-0.0656	*PsbS1* (Os01g0869800)
3	qA_{400}/A_{1800} 4.1	4	4,230,805	ud4001319	15,944,977	18,706,317	8.50	12.56	-0.0456	*VDE*(Os04g0379700)
4	qA_{400}/A_{1800} 8.1	8	8,983,572	SNP-8.26378199.	25,757,847	26,380,914	3.21	3.86	-0.0258	*OsPGRLIA* (Os08g0526300)
5	qA_{400}/A_{1800} 9.1	9	9,711,583	SNP-9.18053834.	16,505,404	18,054,836	9.91	13.94	-0.051	*OsbZIP72* (Os09g0456200)

RuBP active site, preventing starch biosynthesis (Levey et al. 2019). It has already been reported that photorespiration in C3 plants protects from photooxidation, but lower expression of PGLP may reduce the 40% reduction of photosynthesis (Kozaki & Takeba, 1996; Levey et al., 2019). Thus, limiting the photorespiration of RuBP helps the relaxation of NPQ indirectly. So, PGLP2 also has some role in improving the carboxylation efficiency of RuBP; the event finally helps in photoprotection recovery quickly.

The gene LUT2/LYCE, Lycopene epsilon cyclase, Os01g0581300, is an essential enzyme responsible for producing the most abundant Xanthophyll species, lutein. It is the most abundant xanthophyll in plants and helps quench overexcited chlorophyll, preventing reactive oxygen species ($^1O_2$). Its role in ROS scavenging is well known. *OsLUT1A* and *OsLUT2* were also reported as the genes near the NPQ-associated marker locus in rice (Wang et al. 2017). Violaxanthin, another carotenoid, also scavenges toxic singlet oxygen $^1O_2$, which protects thylakoidal proteins, and in excess light, violaxanthin is de-epoxidised by the gene VDE to produce zeaxanthin. Contrarily, when light intensity becomes normal, i.e., less than 1000 µmol/m^2/s PPDF, quicker epoxidation of zeaxanthin leads to violaxanthin conversion, i.e., relaxation of NPQ which finally helps photoprotection recovery (Kromdijk et al. 2016; Vaz and Sharma, 2009). Although the conversion of zeaxanthin to violaxanthin requires a relatively long period of 5–10 min (Bassi et al., 2021), the association of both VDE and ZEP with the A_{400}/A_{1800} ratio measure in five-minute intervals confirms their role in quick photoprotection recovery in other ways. When plants receive more than optimum light intensity, excitation pressure in the antenna rises, the photosynthetic chain saturates, and thylakoid lumen pH decreases (through an increase in proton pumping). Acidifying the thylakoid lumen triggers protonation of PsbS protein and de-epoxidation of violaxanthin to antheraxanthin and zeaxanthin via the xanthophyll cycle. This protonated PsbS1, which causes a conformational change in PSII-LHCII super complex (PSII-LHCII sc) and accumulation of xanthophylls (zeaxanthin and lutein) induce feedback deexcitation, qE and qZ components (Kromdijk et al. 2016; Fu et al. 2021; Moya Clark 2023; Bassi et al., 2021). In this study, a heat shock protein is associated with an A_{400}/A_{1800} ratio with other PP-related genes, which needs further study regarding its role in PP. A critical component of photoprotection is heat emission from the chlorophyll overexcitation that helps it regain its photoharvesting state. Whether the identified heat shock protein on chromosome 6 at the position of 15,578,047–15,582,320 nt has any role needs to be deciphered by developing the near-isogenic line and site-directed mutagenesis study.

The *PsbS1* is a well-known protein responsible for a wide range of nonphotochemical quenching (NPQ) and quick photoprotection recovery, which was not identified in GWAS. In an earlier study, no association was observed with a particular subpopulation, like, indica, japonica and aus (Wang et al. 2017). It is due to the lack of polymorphism in *PsbS1* and its surrounding sequence within a subpopulation. In the studied panel, no japonica subtypes are included in genotypes, which may be one reason for the non-association of the *PsbS1* locus. However, in QTL analysis, a major QTL carrying the *PsbS1* gene (Os01g0869800), identified in this study, explained almost 25% of the total variation. The other QTL on chromosome 4 carries the *OsVDE* (Os04g0379700) gene, also identified in GWAS. Like earlier studies reported the role of xanthophyll cycle genes in photoprotection recovery, our study confirmed the same locus in GWAS and QTL analysis.

The mapping of the instantly measured A_{400}/A_{1800} ratio identified the loci with known candidate genes of photoprotection recovery or NPQ like *OsPsbS1*, *OsVDE*, *OsZEP*, *OsLUT2*, *OsPGRL1A*, *OsPGLP2*. The qE component accounts for 80% of NPQ and can recover, primarily within a short period; exploiting this component for faster restoration of the maximum efficiency of CO_2 assimilation might be the main cause of the strong association between A_{400}/A_{1800} and quick photoprotection recovery. Like quick photoprotection recovery, the A_{400}/A_{1800} ratio is significantly associated with biomass and yield in a RIL population. The *PsbS1* allele of Swarnaprabha can be targeted to enhance the yield potentiality of rice, particularly in regions where low and fluctuating light is a problem, like Eastern India.

Conclusion

The instantly measured A_{400}/A_{1800} ratio in 8–10 days rice flag leaf can be an alternative to the time-consuming and cumbersome phenotyping of photoprotection recovery in rice, particularly for screening a large number of genotypes or segregants.

Supplementary Information

The online version contains supplementary material available at https://doi.org/10.1186/s12284-024-00739-3.

Supplementary Material 1

Supplementary Material 2

Supplementary Material 3

Acknowledgements
ICAR Incentivizing Scheme.

Author Contributions
SS, NS and SB designed the experiment and analysed the data. SS, NS, KB, RK, SG, SG, NK, TKB and PKB performed all experiments. SB wrote the manuscript with the assistance of SS.

Funding
ICAR, Government of India.

Data Availability
All data generated or analysed during this study are included in this published article and its supplementary information files (Supplementary Tables 1 to 7), including SNP-based genotyping data in an association panel and a RIL population in Supplementary Tables 6 and Supplementary Table 7.

Declarations

Ethics Approval and Consent to Participate
The manuscript does not report on or involve the use of any animal or human data or tissue.

Materials and Experimental Statements
All the genotypes used in this study are either released varieties or indigenous rice of Bengal maintained in the University's Crop Research Unit field gene bank, where permissions or licenses are not required as they were not used for commercial purposes. All experimental procedures were conducted following the guidelines.

Consent for Publication
Not Applicable.

Competing Interests
The authors declare no competing interests.

Received: 25 June 2024 / Accepted: 30 August 2024
Published online: 16 September 2024

References

Abdullah AB, Ito S, Adhana K (2006), March Estimate of rice consumption in Asian countries and the world towards 2050. In *Proceedings for Workshop and Conference on Rice in the World at Stake* (Vol. 2, pp. 28–43)
Acevedo- Siaca L, Coe R, Wang Y, Kromdijk J, Quick WP, Long SP (2020) Variation in photosynthetic induction between rice accessions and its potential for improving productivity. New Phytol 227:1097–1108
Acevedo-Siaca LG, DionoraJ, Laza R, Paul QW, Long SP (2021) Dynamics of photosynthetic induction and relaxation within the canopy of rice and two wild relatives. Food Energy Secur 10:e286
Ambavaram MM, Basu S, Krishnan A, Ramegowda V, Batlang U, Rahman L, Pereira A (2014) Coordinated regulation of photosynthesis in rice increases yield and tolerance to environmental stress. Nat Commun 5(1):5302
Amin MW, Aryan S, Habibi N, Kakar K, Zahid T (2022) Elucidation of photosynthesis and yield performance of rice (*Oryza sativa* L.) under drought stress conditions. Plant Physiol Rep 27(1):143–151
Bassi R, Dall'Osto L (2021) Dissipation of light energy absorbed in excess: the molecular mechanisms. Annu Rev Plant Biol 72:47–76
De Souza AP, Burgess SJ, Doran L, Hansen J, Manukyan L, Maryn N, Long SP (2022) Soybean photosynthesis and crop yield are improved by accelerating recovery from photoprotection. Science 377(6608):851–854
Earl DA, VonHoldt BM (2012) STRUCTURE HARVESTER: a website and program for visualizing STRUCTURE output and implementing the Evanno method. Conserv Genet Resour 4:359–361
Fischer RA, Edmeades GO (2010) Breeding and cereal yield progress. Crop Sci 50:S–85
Foyer C, Ruban A, Nixon P (2017) Enhancing photosynthesis in crop plants: targets for improvement. Philosophical Trans Royal Soc B Biol Sci, *372*(1730)
Fu X, Liu C, Li Y, Liao S, Cheng H, Tu Y, Wang G (2021) The coordination of OsbZIP72 and OsMYBS2 with reverse roles regulates the transcription of OsPsbS1 in rice. New Phytol 229(1):370–387
Ganguly S, Saha S, Vangaru S, Purkayastha S, Das D, Saha AK, Bhattacharyya S (2020) Identification and analysis of low light tolerant rice genotypes in field conditions and their SSR-based diversity in various abiotic stress tolerant lines. J Genet 99:1–9
Giovagnetti V, Ruban AV (2015) Discerning the effects of photoinhibition and photoprotection on the rate of oxygen evolution in Arabidopsis leaves. J Photochem Photobiol B 152:272–278
Hill WG, Weir BS (1988) Variances and covariances of squared linkage disequilibria in finite populations. Theor Popul Biol 33(1):54–78
Huang M, Liu X, Zhou Y, Summers RM, Zhang Z (2019) BLINK: a package for the next level of genome-wide association studies with both individuals and markers in the millions. Gigascience 8(2):giy154
Jonik C, Sonnewald U, Hajirezaei MR, Flügge UI, Ludewig F (2012) Simultaneous boosting of source and sink capacities doubles tuber starch yield of potato plants. Plant Biotechnol J 10(9):1088–1098
Kasajima I, Ebana K, Yamamoto T, Takahara K, Yano M, Kawai-Yamada M, Uchimiya H (2011) Molecular distinction in genetic regulation of nonphotochemical quenching in rice. Proc Natl Acad Sci 108(33):13835–13840
Kozaki A, Takeba G (1996) Photorespiration protects C3 plants from photooxidation. Nature 384(6609):557–560
Kromdijk J, Głowacka K, Leonelli L, Gabilly ST, Iwai M, Niyogi KK, Long SP (2016) Improving photosynthesis and crop productivity by accelerating recovery from photoprotection. Science 354(6314):857–861
Levey M, Timm S, Mettler-Altmann T, Luca Borghi G, Koczor M, Arrivault S, PM Weber A, Bauwe H, Gowik U, Westhoff P (2019) Efficient 2-phosphoglycolate degradation is required to maintain carbon assimilation and allocation in the C4 plant Flaveria bidentis. J Exp Bot 70(2):575–587
Liu X, Huang M, Fan B, Buckler ES, Zhang Z (2016) Iterative usage of fixed and random effect models for powerful and efficient genome-wide association studies. PLoS Genet, 12(2), e1005767
Long SP, ZHU XG, Naidu SL, Ort DR (2006) Can improvement in photosynthesis increase crop yields? Plant Cell Environ 29(3):315–330
Makino A (2021) Photosynthesis improvement for enhancing productivity in rice. Soil Sci Plant Nutr 67(5):513–519
Matuszyńska A, Heidari S, Jahns P, Ebenhöh O (2016) A mathematical model of non-photochemical quenching to study short-term light memory in plants. Biochim et Biophys Acta (BBA)-Bioenergetics 1857(12):1860–1869
Meng L, Li H, Zhang L, Wang J (2015) QTL IciMapping: Integrated software for genetic linkage map construction and quantitative trait locus mapping in biparental populations. Crop J 3(3):269–283
Money D, Gardner K, Migicovsky Z, Schwaninger H, Zhong GY, Myles S (2015) LinkImpute: fast and accurate genotype imputation for nonmodel organisms. G3: Genes Genomes Genet 5(11):2383–2390
Morales KY, Singh N, Perez FA, Ignacio JC, Thapa R, Arbelaez JD, Thomson MJ (2020) An improved 7K SNP array, the C7AIR, provides a wealth of validated SNP markers for rice breeding and genetics studies. PLoS One 15(5):e0232479
Moya Clark ID (2023) *Structural insights into PsbS and its interactions with the PSII-LHCII supercomplex under active and inactive nonphotochemical states in Spinacia oleracea* (Master's thesis)

Muhammad I, Shalmani A, Ali M, Yang QH, Ahmad H, Li FB (2021) Mechanisms regulating the dynamics of photosynthesis under abiotic stresses. Front Plant Sci 11:615942
Muller P, Li XP, Niyogi KK (2001) Non-photochemical quenching. A response to excess light energy. Plant Physiol 125(4):1558–1566
Murchie EH, Lawson T (2013) Chlorophyll fluorescence analysis: a guide to good practice and understanding some new applications. J Exp Bot 64(13):3983–3998
Oxborough K, Baker NR (1997) Resolving chlorophyll a fluorescence images of photosynthetic efficiency into photochemical and non-photochemical components–calculation of qP and Fv-/Fm-; without measuring Fo. Photosynth Res 54:135–142
Pritchard JK, Stephens M, Donnelly P (2000) Inference of population structure using multilocus genotype data. Genetics 155(2):945–959
Reynolds M, Foulkes MJ, Slafer GA, Berry P, Parry MA, Snape JW, Angus WJ (2009) Raising yield potential in wheat. J Exp Bot 60(7):1899–1918
Rochaix JD (2007) Role of thylakoid protein kinases in photosynthetic acclimation. FEBS Lett 581(15):2768–2775
Rossi M, Bermudez L, Carrari F (2015) Crop yield: challenges from a metabolic perspective. Curr Opin Plant Biol 25:79–89
Ruban AV (2016) Nonphotochemical chlorophyll fluorescence quenching: mechanism and effectiveness in protecting plants from photodamage. Plant Physiol 170(4):1903–1916
Ruban AV, Murchie EH (2012) Assessing the photoprotective effectiveness of non-photochemical chlorophyll fluorescence quenching: a new approach. Biochim et Biophys Acta (BBA)-Bioenergetics 1817(7):977–982
Saha S, Purkayastha S, Nimitha K, Ganguly S, Das S, Ganguly S, Bhattacharyya S (2023) Rice (Oryza sativa) alleviates photosynthesis and yield loss by limiting specific leaf weight under low light intensity. Funct Plant Biol 50(4):267–276
Smith MR, Rao IM, Merchant A (2018) Source-sink relationships in crop plants and their influence on yield development and nutritional quality. Front Plant Sci 9:420465
Sonnewald U, Fernie AR (2018) Next-generation strategies for understanding and influencing source–sink relations in crop plants. Curr Opin Plant Biol 43:63–70
Takahashi S, Badger MR (2011) Photoprotection in plants: a new light on photosystem II damage. Trends Plant Sci 16(1):53–60
Thomson MJ, Singh N, Dwiyanti MS, Wang DR, Wright MH, Perez FA, McCouch SR (2017) Large-scale deployment of a rice 6 K SNP array for genetics and breeding applications. Rice 10(1):1–13
Tietz S, Hall CC, Cruz JA, Kramer DM (2017) *NPQ (T): a chlorophyll fluorescence parameter for rapid estimation and imaging of non-photochemical quenching of excitons in photosystem-II-associated antenna complexes* (Vol. 40, No. 8, pp. 1243–1255)
Vaz J, Sharma PK (2009) Photoinhibition and photosynthetic acclimation of rice (Oryza sativa L. cv Jyothi) plants grown under different light intensities and photoinhibited under field conditions. Indian J Biochem Biophys 46(3):253–260
Vos PG, Paulo MJ, Voorrips RE, Visser RG, van Eck HJ, van Eeuwijk FA (2017) Evaluation of LD decay and various LD-decay estimators in simulated and SNP-array data of tetraploid potato. Theor Appl Genet 130:123–135
Wang Q, Zhao H, Jiang J, Xu J, Xie W, Fu X, Wang G (2017) Genetic architecture of natural variation in rice nonphotochemical quenching capacity revealed by genome-wide association study. Front Plant Sci 8:1773

Publisher's Note